

# OPTIMIZING THE ENVIRONMENTAL FACTORS FOR THE AFFINITY OF $^{222}\text{Rn}$ WITH CARBON FIBERS

## OPTIMIZACIJA OKOLJSKIH FAKTORJEV ZA POVEČANJE AFINITETE $^{222}\text{Rn}$ NA OGLJIKOVH VLAKNH

Yeon Ji Cho, Woo Seok Cho, Sang Sun Choi\*

Department of Environmental and Energy Engineering, Anyang University, Anyang 14028, South Korea

Prejem rokopisa – received: 2021-04-21; sprejem za objavo – accepted for publication: 2021-05-04

doi:10.17222/mit.2021.145

Radon ( $^{222}\text{Rn}$ ) is a member of the decay chain of  $^{238}\text{U}$ . It has been well documented that  $^{222}\text{Rn}$  is known to present a risk of lung cancer once inhaled. For practical implementation, this study makes use of activated carbon fibers (ACFs) to uptake  $^{222}\text{Rn}$  through environmental variations in the temperature, dosage of the adsorbent and circulate conditions. Here, three ACF samples were prepared via different carbonization and activation temperatures from 850 °C to 900 °C. The observed adsorption characteristics show that low temperature and high surface contact of an adsorbent with rich micropores allow the maximum adsorption of  $^{222}\text{Rn}$ . No such correlation was observed in the case of increasing the circulate conditions. However, there was a direct influence on the maximum adsorption capacity once the circulate conditions decreased. In summary, these findings expand the understanding of the adsorption, dependency on the factors and a proper carbonaceous-material design for reducing  $^{222}\text{Rn}$ .

Keywords: radon, carbon fibers, temperature, surface contact, pressure, flow rate

Radon ( $^{222}\text{Rn}$ ) je člen v verigi radioaktivnega razpada  $^{238}\text{U}$ . Dobro je znano in dokumentirano, da njegovo inhaliranje predstavlja nevarnost za nastanek pljučnega raka. V članku avtorji predstavljajo praktične možnosti implementacije aktiviranih ogljikovih vlaken (ACFs) za adsorpcijo  $^{222}\text{Rn}$  in razumevanje vplivov okolja, kot so: sprememba temperature, doza adsorbenta in pogoji cirkulacije (pretoka zraka). Avtorji so pripravili vzorce ACF pri različnih pogojih karbonizacije in temperaturah aktivacije med 850 °C in 900 °C. Opazovanje adsorpcijskih karakteristik je pokazalo, da je za maksimalno kapaciteto adsorpcije  $^{222}\text{Rn}$  potrebna nizka temperatura aktivacije in visok površinski kontakt adsorbenta z bogatim številom mikropor. Ta povezava pa ni bila ugotovljena v primeru povečane cirkulacije. Vendar pa avtorji ugotavljajo, da na maksimalno adsorpcijsko kapaciteto vpliva zmanjšana cirkulacija. Zaključujejo z ugotovitvijo, da je pričujoča raziskava razširila razumevanje osnov adsorpcije radioaktivnega radona, pokazala na njeno odvisnost od vplivnih faktorjev in našla primerno obliko materiala na osnovi ogljika, ki lahko zmanjša vsebnost  $^{222}\text{Rn}$  v okolju.

Gljučne besede: radon, ogljikova vlakna, temperatura, površinski kontakt, tlak, pretok

## 1 INTRODUCTION

Radon ( $^{222}\text{Rn}$ ) is a noble radioactive gas that emanates from the decay of  $^{238}\text{U}$  with a half-life of less than 4 days. The infiltration of  $^{222}\text{Rn}$  with its high mobility is considered to be the most significant cause of indoor radon exposure.<sup>1</sup> Epidemiological studies have shown that residential radon exposure may cause lung cancer even at low radon levels.<sup>2–5</sup> In this sense, an efficient uptake of  $^{222}\text{Rn}$  becomes quintessential. The use of activated carbons was first introduced in 1906 by Rutherford and flourished for decades in response to the above need.<sup>6</sup> Activated carbon is widely applied in both gas and liquid-phase adsorbents due to its relatively low cost, high porosity and electric independence. However, adsorbate  $^{222}\text{Rn}$  molecules first need to pass through macro- and mesopore regions before entering micropore regions because of their ladder-like structure. Due to the natural promiscuity of activated carbon, activated carbon fibers (ACFs) can be an excellent alternative adsorbent since microporous characteristics allow  $^{222}\text{Rn}$  to bypass macro-

and mesopore regions and directly reach micropore regions.<sup>7–10</sup> Using ACFs can also be ideal for minimizing the waste disposal during the material synthesis by using the pitch from the oil-industrial sector as the precursor. Inspired by the above encouraging characteristics, we synthesized pitch-based ACFs as an adsorbent for the  $^{222}\text{Rn}$  adsorption. Here, surface characteristics of samples, including temperatures and circulate conditions, were determined as experimental variations. While previous studies merely observed the affinity of  $^{222}\text{Rn}$  with carbonaceous materials via surface areas, our work further explores the trinity of environmental factors for a better understanding.<sup>11</sup> These findings may advance the fundamental knowledge of the  $^{222}\text{Rn}$  uptake using carbonaceous materials for an efficient design of adsorbents.

## 2 EXPERIMENTAL PART

Pyrolysis fuel oil was kindly supplied by Hyundai Oilbank and used as the precursor. The synthesis of ACFs was prepared using pyrolysis fuel oil. First, the temperature was elevated from room temperature to 300 °C under  $\text{N}_2$  atmosphere (2 L/min) for 1 h to remove

\*Corresponding author's e-mail:  
choiss@anyang.ac.kr (Sang Sun Choi)

all the unnecessary impurities. Afterward, the material was spun in a centrifugal spinneret at a temperature of 245 °C. The resulting carbon fibers were then stabilized in air at 260 °C for another 5 h. For the carbonization and activation, carbon fibers were heated under  $\text{N}_2$  (4 L/min) and  $\text{H}_2\text{O}$  atmosphere (0.2 mL/min) for 1 h, respectively, in a tubular furnace. Herein, temperature ranges from (850, 875 and 900) °C were designated for carbonization and activation to observe the correlation between the specific surface of samples and the adsorption capacity. We further denoted the samples by their carbonization and activation temperatures: ACF850, ACF875 and ACF900 for convenience.

The  $^{222}\text{Rn}$  measurement was conducted using passivated implanted planar silicon sensors adapted to RAD-7 (DurrIDGE) at room temperature for 48 h. As illustrated in **Figure 1**, a parent nuclide ( $^{226}\text{Ra}$ ) was introduced to lure  $^{222}\text{Rn}$  inside the chamber. Each sample was heated at 90 °C for 3 h before the  $^{222}\text{Rn}$  measurement and the inner-atmosphere was circulated by designated conditions (a pressure of  $-0.02 - 0.02$  MPa and a flow rate of 1–5 L/min). Physical characteristics of the samples were determined using ASAP 2460 (Micromeritics). The specific surface area ( $S_{\text{BET}}$ ) was calculated with the Brunauer-Emmett-Teller (BET) method. The micropore area ( $S_{\text{M}}$ ) and the external area ( $S_{\text{E}}$ ) were evaluated with the Barrett-Joyner-Halenda (BJH) method using a  $\text{N}_2$  adsorption isotherm. A CHN/S analyzer was employed to determine the contents of carbon, hydrogen and nitrogen using 2400 I (Perkin Elmer). Here, the oxygen content was calculated on the basis of the difference between the carbon, hydrogen and nitrogen contents. Scanning-electron-microscope images were observed under an accelerating voltage of 20 kV using S-3000H (Hitachi).

### 3 RESULTS AND DISCUSSION

**Tables 1** and **2** list the properties of the samples. As the temperature increased from 850 °C to 875 °C, there

was a corresponding increase in both  $S_{\text{BET}}$  (21.96 %) and  $S_{\text{M}}$  (36.28 %). The dependency of  $S_{\text{BET}}$  and  $S_{\text{M}}$  on the temperature was reduced from 900 °C onwards. The maximum values for  $S_{\text{BET}}$  and  $S_{\text{M}}$  were  $1653 \text{ m}^2\cdot\text{g}^{-1}$  and  $1447 \text{ m}^2\cdot\text{g}^{-1}$  at 875 °C, respectively. In all the cases, carbonaceous samples in the fiber form revealed a decent amount of micropores. It is also worth pointing out that the decrease in the C- and H-contents after the activation could be attributed to the dehydrogenation of linear structures to form an aromatic carbon network (**Figure 2a**). O-contents, in other words, surface functional groups (viz., carboxylic, lactonic and phenolic) were in the order of  $\text{ACF875} > \text{ACF900} > \text{ACF850}$ . This may account for the high textual properties of ACF875, which allow further integration of O-contents before and/or even after the fabrication once the surface is exposed to air (**Figure 2b**).<sup>12</sup> Irrespective of whether the N- or S-contents vary insignificantly, the aforementioned data set consistently suggests that ACF875 with the highest physicochemical properties may reveal the highest  $^{222}\text{Rn}$  adsorption capacity among the samples.

**Table 1:** Textural properties of the samples using  $\text{N}_2$  adsorption isotherm

Sample	$S_{\text{BET}}/\text{m}^2\cdot\text{g}^{-1}$	$S_{\text{M}}/\text{m}^2\cdot\text{g}^{-1}$	$S_{\text{E}}/\text{m}^2\cdot\text{g}^{-1}$
ACF850	1290	922	368
ACF875	1653	1447	206
ACF900	1424	1108	316

**Table 2:** Elemental compositions of the samples (w/%)

Sample	C	H	N	S	O (difference)
ACF850	94.32	0.24	0.15	0.02	5.27
ACF875	91.65	0.09	0.16	0.01	8.09
ACF900	93.41	0.17	0.15	0.02	6.25

The adsorption capacity of  $^{222}\text{Rn}$  under various conditions of temperature and sample dosage was investigated each time under a pressure of  $-0.02$  MPa and flow rate of 1 L/min, respectively (**Figure 3**). Given that a simulta-

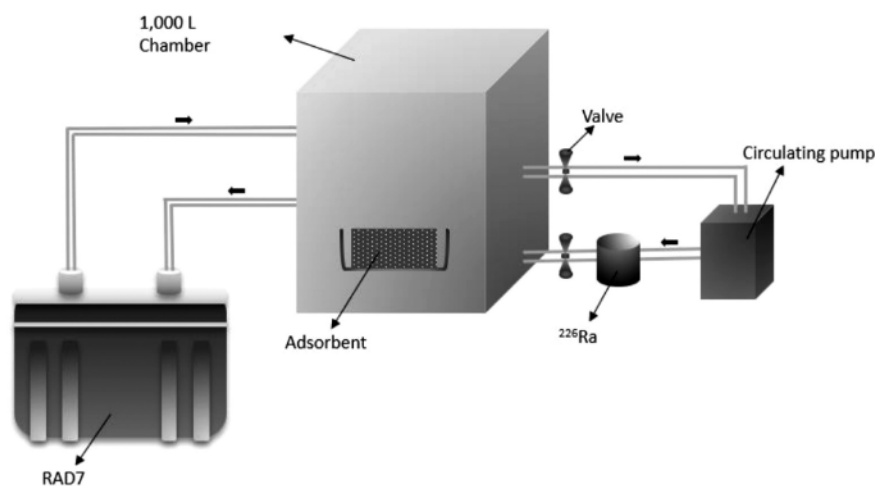


**Figure 1:** Measurement apparatus for  $^{222}\text{Rn}$  adsorption capacity

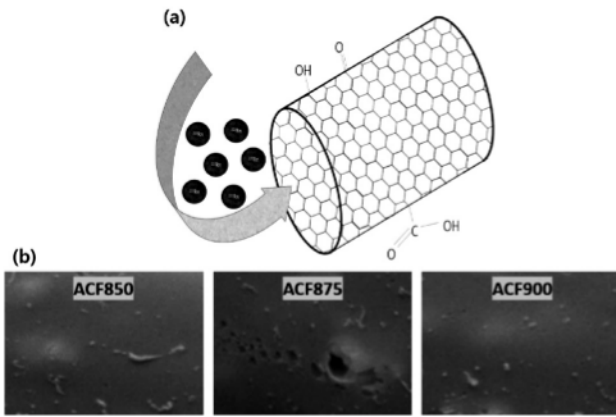


Figure 2: a) Possible structural representation of  $^{222}\text{Rn}$  adsorption process; b) sample morphology observed with a scanning electron microscope with a given magnitude of  $\times 10\text{ K}$

neous removal has practical applicability, up to 48 h was suggested as the maximum time frame. Concomitantly, a natural decay plot is also included in dark blue. The vari-

ation in the temperature suggests that ACF850 and ACF900 showed a much faster  $^{222}\text{Rn}$  adsorption within 0–36 h, as exemplified by robust surface characteristics of meso- and macropores. After 36 h, while again no significant adsorption capacity was identified in ACF850 and ACF900, plots of ACF875 showed a drastic shift due to a continuous accumulation of  $^{222}\text{Rn}$  onto micropores. Based on the physicochemical properties, we assumed that ACF875 would have the most  $^{222}\text{Rn}$  adsorption capacity.

Calculating the values from Figure 3c, the final adsorption capacity was in the order of ACF875 ( $135.2\text{ Bq/m}^3$ ) > ACF900 ( $141.1\text{ Bq/m}^3$ ) > ACF850 ( $148.1\text{ Bq/m}^3$ ). This order can be found in relevant adsorption studies using porous media.<sup>13,14</sup> The temperature was in an inversely proportional correlation with the adsorption capacity in all the cases except for ACF875. This is in accordance with the previous studies, suggesting that the  $^{222}\text{Rn}$  adsorption coefficient at zero temperature shows an exponential increase.<sup>15</sup> This observation is also consistent with the variation in the sample dosage,

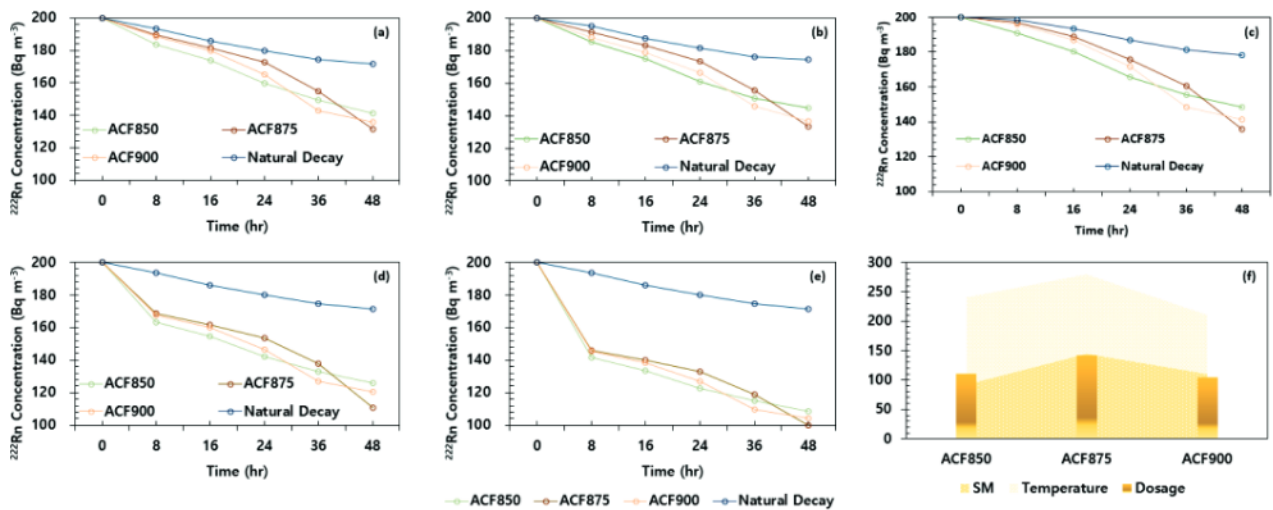


Figure 3: Linearized plots of  $^{222}\text{Rn}$  breakthrough due to the temperature and sample dosage: a)  $25^\circ\text{C} - 20\text{ g}$ , b)  $30^\circ\text{C} - 20\text{ g}$ , c)  $35^\circ\text{C} - 20\text{ g}$ , d)  $25^\circ\text{C} - 25\text{ g}$ , e)  $25^\circ\text{C} - 30\text{ g}$ , f) correlation between micropores ( $\text{SM}$ ;  $10^{-1} S_M$ ), temperature ( $35^\circ\text{C}$ ) and sample dosage ( $30\text{ g}$ ) in the case of the maximum adsorption capacity

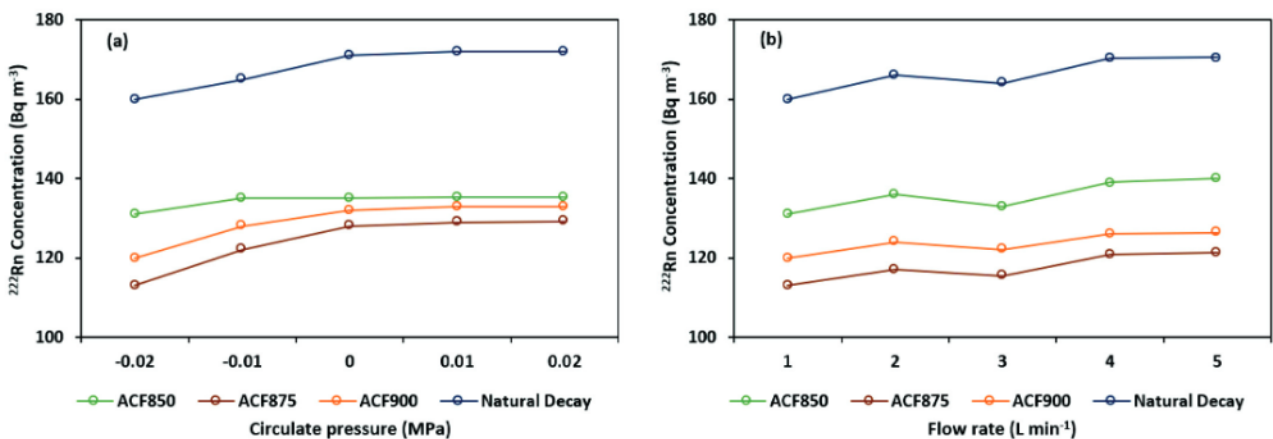


Figure 4: Linearized plots of  $^{222}\text{Rn}$  breakthrough as a function of: a) circulate pressure, b) flow rate, using 20-g samples at  $25^\circ\text{C}$  for 48 h

showing that ACF875 had a slow start but ended up with the highest adsorption capacity of <sup>222</sup>Rn. According to the data acquired from **Figure 3e**, the final adsorption capacity was in the order of ACF875 (100.01 Bq/m<sup>3</sup>) > ACF900 (104.41 Bq/m<sup>3</sup>) > ACF850 (108.72 Bq/m<sup>3</sup>). The data from these experiments also allows us to compare the environments affecting the effective <sup>222</sup>Rn adsorption. Though the surface geology of ACFs first seemed to imbibe <sup>222</sup>Rn via micropores, different proportions of micropores of each sample resulted in an unpredictable adsorption capacity within a long-term scenario. It should also be noted that the sample dosage showed a greater influence than the temperature in all the cases (**Figure 3f**). Given that the variation in the sample dosage may be insufficient for the <sup>222</sup>Rn adsorption capacity over 50 %, a chemical modification of the surface or the use of other material-based adsorbents may further increase the numerical values of adsorption.

According to the relevant literature, circulate pressure is in a liner correlation with the adsorption capacity.<sup>16</sup> In the case of <sup>222</sup>Rn, a decrease in the circulate pressure may enhance the overall flux as shown by early experiments.<sup>17–18</sup> A comparison of the <sup>222</sup>Rn adsorption capacity with 20-g samples at a flow rate of 1 L/min over 48 h is summarized in **Figure 4a**. The adsorbed values of <sup>222</sup>Rn at a low circulate pressure appear to be high because of the enhanced flux. The observed value of ACF875 (114.63 Bq/m<sup>3</sup>) at –0.02 MPa is comparable to that of ACF900 (119.95 Bq/m<sup>3</sup>), but the values in the cases of ACF850 (131.56 Bq/m<sup>3</sup>) and natural decay (160.34 Bq/m<sup>3</sup>) are higher. Likewise, the <sup>222</sup>Rn adsorption is higher at a low flow rate (–0.02 MPa) compared to the values of –0.01–0.02 MPa (**Figure 4b**).<sup>19</sup> This is mainly due to the competition between the surrounding radioactive species and the limited surface pores. From the above results, it can be concluded that all the prepared samples show increased values of <sup>222</sup>Rn adsorption capacity at low temperatures, high contact surfaces, low pressures and high flow rates.

#### 4 CONCLUSION

It is clear from the results of our experiments that a combination of factors including the temperature, contact surface and circulate conditions can effectively enhance the uptake of <sup>222</sup>Rn. Comparable though less pronounced measures are also available for enhancing the adsorption capacity of <sup>222</sup>Rn such as various chemical modifications of the surface of an adsorbent. In summary, with the above calculations and observations, we de facto identified the adsorption mechanisms of <sup>222</sup>Rn and may continue our research in terms of an efficient adsorbent design.

#### Acknowledgements

This work was supported by the Korean Energy Technology Evaluation and Planning (Project No. 20171520000300).

#### Declaration of interest

The authors declare that there is no conflict of interest.

#### 5 REFERENCES

- A. S. Berens, J. Diem, C. Stauber, D. Dai, S. Foster, R. Rothenberg, The use of gamma-survey measurements to better understand radon potential in urban areas, *Sci. Total Environ.*, 31 (2017) 607–608, 888–899, doi:10.1016/j.scitotenv.2017.07.022
- S. Sharma, A. Kumar, R. Mehra, M. Kaur, R. Mishra, Assessment of progeny concentrations of <sup>222</sup>Rn/<sup>220</sup>Rn and their related doses using deposition-based direct progeny sensors, *Environ. Sci. Pollut. Res.*, 25 (2018) 12, 11440–11453, doi:10.1007/s11356-018-1414-7
- B. K. Sahoo, B. K. Sapra, J. J. Gaware, S. D. Kanse, Y. S. Mayya, A model to predict radon exhalation from walls to indoor air based on the exhalation from building material samples, *Sci. Total Environ.*, 13 (2011) 409, 2635–2641. doi:10.1016/j.scitotenv.2011.03.031
- I. V. Yarmoshenko, G. P. Malinovsky, Lung cancer mortality and radon exposure in Russia, *Nukleonika*, 61 (2016) 3, 263–268, doi:10.1515/nuka-2016-0044
- P. Carta, P. Cocco, G. Picchiri, Lung cancer mortality and airways obstruction among metal miners exposed to silica and low levels of radon daughters, *Am. J. Ind. Med.*, 25 (1994) 4, 489–506. doi:10.1002/ajim.4700250404
- J. H. Lee, S. H. Lee, D. H. Suh, Using nanobubbled carbon dioxide for effective microextraction of heavy metals, *J. CO<sub>2</sub> Util.*, 39 (2020), 101163, doi:10.1016/j.jcou.2020.101163
- H. Chen, K. Lv, Y. Du, H. Ye, D. Du. Microwave-assisted rapid synthesis of Fe<sub>2</sub>O<sub>3</sub>/ACF hybrid for high efficient As (V) removal, *J. Alloys Compd.*, 674 (2016), 399–405, doi:10.1016/j.jallcom.2016.03.024
- J. Duan, H. Ji, T. Xu, F. Pan, X. Liu, W. Liu, D. Zhao, Simultaneous adsorption of uranium (VI) and 2-chlorophenol by activated carbon fiber supported/modified titanate nanotubes (TNTs/ACF): Effectiveness and synergistic effects, *Chem. Eng. J.*, 406 (2021), 126752, doi:10.1016/j.ccej.2020.126752
- J. H. Lee, S. H. Lee, D. H. Suh, CO<sub>2</sub> treatment of carbon fibers improves adsorption of fuel cell platinum, *Environ. Chem. Lett.*, 1–6 (2020), doi:10.1007/s10311-020-01105-7
- M. Annamalai, R. Ramasubbu, Optimizing the formulation of E-glass fiber and cotton shell particles hybrid composites for their mechanical behavior by mixture design analysis, *Mater. Technol.*, 52 (2018) 2, 207–14, doi:10.17222/mit.2017.119
- D. C. Gwak, S. S. Choi, J. H. Lee, S. H. Lee, Synthesis and Characterization of Pitch-Based Activated Carbon Fiber for Indoor Radon Removal, *Nucl. Fuel. Cycle. Waste. Technol.*, 15 (2017) 3, 207–218, doi:10.7733/jnfcwt.2017.15.3.207
- M. A. A. Zaini, Y. Amano, M. Machida, Adsorption of heavy metals onto activated carbons derived from polyacrylonitrile fiber, *J. Hazard. Mater.*, 180 (2010) 1–3, 552–560, doi:10.1016/j.jhazmat.2010.04.069
- C. Kütahyalı, M. Eral, Selective adsorption of uranium from aqueous solutions using activated carbon prepared from charcoal by chemical activation, *Sep. Purif. Technol.*, 40 (2004) 2, 109–114, doi:10.1016/j.seppur.2004.01.011
- C. Xu, J. Wang, T. Yang, X. Chen, X. Liu, X. Ding, Adsorption of uranium by amidoximated chitosan-grafted polyacrylonitrile, using

- response surface methodology, *Carbohydr. Polym.*, 121 (2015), 79–85, doi:10.1016/j.carbpol.2014.12.024
- <sup>15</sup> L. Guo, Y. Wang, L. Zhang, Z. Zeng, W. Dong, Q. Guo, The temperature dependence of adsorption coefficients of  $^{222}\text{Rn}$  on activated charcoal: an experimental study, *Appl. Radiat. Isot.*, 125 (2017), 185–187, doi:10.1016/j.apradiso.2017.04.023
- <sup>16</sup> H. G. Drickamer, Electronic transitions in transition metal compounds at high pressure, *Angew. Chem. Int.*, 13 (1974) 1, 39–47, doi:10.1002/anie.197400391
- <sup>17</sup> S. Jha, A. H. Khan, U. C. Mishra, A study of the  $^{222}\text{Rn}$  flux from soil in the U mineralised belt at Jaduguda, *J. Environ. Radioact.*, 49 (2000) 2, 157–169, doi:10.1016/S0265-931X(99)00117-4
- <sup>18</sup> Y. Nakano, K. Ichimura, H. Ito, T. Okada, H. Sekiya, Y. Takeuchi, M. Yamashita, Evaluation of radon adsorption efficiency values in xenon with activated carbon fibers, *Prog. Theor. Exp. Phys.*, (2020) 11, 113H01, doi:10.1093/ptep/ptaa119
- <sup>19</sup> Q. Zhou, G. Zhao, D. Xiao, S. Qiu, Q. Lei, K. J. Kearfott, Prediction of radon removal efficiency for a flow-through activated charcoal system and radon mitigation characteristics, *Radiat. Meas.*, 119 (2018), 112–120, doi:10.1016/j.radmeas.2018.10.004